

# 침자극에 의한 안정성 네트워크 변화를 관찰하기 위한 Regional Homogeneity와 Amplitude of Low Frequency Fluctuation의 변화 비교: fMRI연구

여수정<sup>1,2</sup>

<sup>1</sup>경희대학교 동서의학연구소, <sup>2</sup>경희대학교 한의과대학 경혈학교실

## Changes of Regional Homogeneity and Amplitude of Low Frequency Fluctuation on Resting-State Induced by Acupuncture

Sujung Yeo<sup>1,2</sup>

<sup>1</sup>Research Group of Pain and Neuroscience, WHO Collaborating Centre, East-West Medical Research Institute,  
<sup>2</sup>Department of Acupuncture and Meridian, Graduate School of Applied Korean Medicine, Kyung Hee University

**Objectives :** Our study aimed to investigate the sustained effects of sham (SHAM) and verum acupuncture (ACUP) into the post-stimulus resting state. **Methods :** In contrast to previous studies, in order to define the changes in resting state induced by acupuncture, changes were evaluated with a multi-method approach by using regional homogeneity (ReHo) and amplitude of low frequency fluctuation (ALFF). Twelve healthy participants received SHAM and ACUP stimulation right GB34 (Yanglingquan) and the neural changes between post- and pre-stimulation were detected. **Results :** The following results were found; in both ReHo and ALFF, the significant foci of; left and right middle frontal gyrus, left medial frontal gyrus, left superior frontal gyrus, and right posterior cingulate cortex, areas that are known as a default mode network, showed increased connectivity. In addition, in ReHo, but not in ALFF, brain activation changes in the insula, anterior cingulate cortex, and the thalamus, which are associated with acupuncture pain modulation, were found. **Conclusions :** In this study, results obtained by using ReHo and ALFF, showed that acupuncture can modulate the post-stimulus resting state and that ReHo, but not ALFF, can also detect the neural changes that were induced by the acupuncture stimulations. Although more future studies with ReHo and ALFF will be needed before any firm conclusions can be drawn, our study shows that particularly ReHo could be an interesting method for future clinical neuroimaging studies on acupuncture.

**Key words :** fMRI, Regional homogeneity, Amplitude of low frequency fluctuation, Acupuncture, Rest, Post effect

### Introduction

Acupuncture is an ancient therapeutic technique that is

increasingly important as a modality of complementary medicine in Western countries<sup>1,2</sup>. As a result, numerous researchers have studied the effects of acupuncture<sup>3-5</sup>. The devel-

Received June 8, 2013, Revised July 23, 2013, Accepted August 13, 2013

Corresponding author: **Sujung Yeo**

Research Group of Pain and Neuroscience, WHO Collaborating Centre, East-West Medical Research Institute, Department of Acupuncture and Meridian, Graduate School of Applied Korean Medicine, Kyung Hee University, 1 Hoeki-dong, Dongdaemun-gu, Seoul 130-701, Korea  
Tel: +82-2-961-0338, Fax: +82-2-961-7831, E-mail: pinkteeth@khu.ac.kr

This work was supported by the National Research Foundation of Korea(NRF) grant funded by the Korea government(MSIP)(No. 2007-0054931).

© This is an open access article distributed under the terms of the Creative Commons Attribution Non-Commercial License (<http://creativecommons.org/licenses/by-nc/3.0>) which permits unrestricted non-commercial use, distribution, and reproduction in any medium, provided the original work is properly cited.

opment of imaging techniques, such as positron emission tomography (PET) and functional magnetic resonance imaging (fMRI), has provided new tools for researchers to investigate the physiological changes during acupuncture stimulations in humans. Particularly, fMRI is often used since it is a non-invasive technique that can demonstrate the neural changes induced by acupuncture<sup>2,6,7</sup>. In recent years, acupuncture researchers have studied the so called “post-effect” of acupuncture with fMRI. This means that they were not just studying the direct neural responses, but defining the neural changes after acupuncture stimulations. Some clinical reports have indicated that acupuncture efficacy is sustained for some time after removal of the needle(s)<sup>8,9</sup>. Therefore, studies about the post-effect of acupuncture stimulations are very important in order to better understand the neural changes after acupuncture stimulations. Fortunately, with fMRI, the functional changes of resting state connectivity can be evaluated<sup>10,11</sup>, moreover, the post-effect of acupuncture stimulations can also be detected with this resting state connectivity<sup>12-14</sup>.

A review of the literature suggests that resting state connectivity in a default mode network using independent component analysis (ICA), which has been commonly used for depicting functional connectivity within a default mode network in resting-state fMRI studies<sup>15</sup>, can be changed after receiving acupuncture stimulation<sup>7,13,16</sup>. Posterior cingulate cortex (PCC) and precuneus strongly interacted with other brain areas during the pre- and post-stimulation state<sup>14</sup> and there was an increased default mode network with pain (anterior cingulate cortex (ACC), periaqueductal gray), affective (amygdala, ACC), and memory (hippocampal formation, middle temporal gyrus) related brain regions<sup>13</sup>. Study using ReHo also showed the modulation of the medial frontal gyrus, anterior cingulate cortex, precuneus and posterior cingulate cortex which were reported as default mode network induced by acupuncture<sup>17</sup>. In this fMRI study on acupuncture, in line with previous research, the post-effect of acupuncture was studied.

To investigate the sustained effects of acupuncture into post-stimulus rest; changes of regional homogeneity (ReHo),

which measures the temporal similarity of voxels within a given cluster in a voxel-wise fashion<sup>18</sup> and amplitude of low frequency fluctuation (ALFF)<sup>19,20</sup>, which quantifies the strength of the fluctuations in each voxel, on “resting-state networks” were evaluated.

ReHo and ALFF are also methods to detect the resting state network, and many studies have already been done<sup>19-22</sup>, however, to the knowledge of the authors, a comparison on neural changes induced by acupuncture using these methods, has not been demonstrated yet.

This study aimed to investigate the changes in resting state networks after sham (SHAM) and verum acupuncture (ACUP) with ReHo and ALFF. It was hypothesized that acupuncture would modulate post-stimulus rest in a multi-method approach. Moreover, it was expected that both ReHo and ALFF are suitable methods in order to create a deeper insight in the changes in the resting-state brain network induced by acupuncture. Finally, interest was raised in the question; which method (ReHo or ALFF) is most suitable for future clinical neuroimaging research on acupuncture, for instance, for studies on pain modulation<sup>7</sup>?

To address these questions, the following hypothesis was formulated: If acupuncture can modulate resting state connectivity in a default mode network using ICA, then it can also modulate resting state connectivity in a default mode network using ReHo and ALFF.

## Materials and Methods

### 1. Target population

Twelve healthy participants entered our study, six were males and six were females, and their ages ranged from 35 to 71 (mean age  $56.4 \pm 9.8$ ). They were without any neurological or psychiatric history and were right-handed as verified by the Edinburgh Handedness Inventory<sup>23</sup>; their mean score was 100% (SD=0%). All participants provided written, informed consent prior to participation in this experiment, which was performed according to the Declaration of Helsinki and was approved by the institutional

review board of the Human Research Committee (KMC IRB 0861-06C3).

## 2. Paradigm

The fMRI paradigm started with a “REST” condition of 4 min. For the “ACUP” and “SHAM”, there were different blocks of 60 s, for which we used either “passive” acupuncture when the needle was only inserted into the skin or “active” acupuncture, for which the needle was not only inserted into the skin and then left in place, but also stimulated. After SHAM and ACUP, another “REST” condition of 4 min followed. The structural images were acquired between SHAM and ACUP. Finally, although the participants were told that the order was randomized, the actual order was SHAM first and ACUP second (Fig. 1)<sup>13</sup>.

## 3. Acupuncture

For ACUP stimulation, an eastern medical doctor with more than 5 years of experience conducted acupuncture on participants, at right Yanglingquan (GB34)<sup>5</sup>, which is on the fibular aspect of the leg, in the depression anterior and distal to the head of the fibula, according to the WHO Standard Point Locations<sup>24</sup>. For ACUP stimulation, the needle (0.25 × 40 mm, Dong Bang Acupuncture Inc.) was manually inserted into the right GB34 to a depth of approximately 1.0 cm, left for 60 s, and rotated bidirectionally at 1 Hz for 60 s, total 60 times, according to the paradigm (Fig. 2).

For SHAM stimulation, a blunt type needle was first used to poke the skin at the right GB34<sup>5</sup>. In contrast to ACUP,

the blunt type needle was not inserted into the skin, but only poked onto the skin. Besides that, the same paradigm was used as for ACUP, and the blunt type needle was also rotated bidirectionally at 1 Hz for 60 s. All participants were informed that two kinds of acupuncture stimulation were used. Moreover, they were informed that the sensation could be somewhat different, but that the two kinds of acupuncture stimulation would have the same effect.

## 4. fMRI data acquisition

A Philips 3.0 T MRI system equipped for echo planer imaging (EPI) was used for data acquisition. For each participant, 120 contiguous EPI functional volumes for “REST” and 150 for “ACUP” and “SHAM” (time repetition [TR]=2,000 ms, time echo [TE]=35 ms, flip angle=90°, slice thickness=4.5, matrix=96×128, field of view [FOV]=230×182×135 mm,

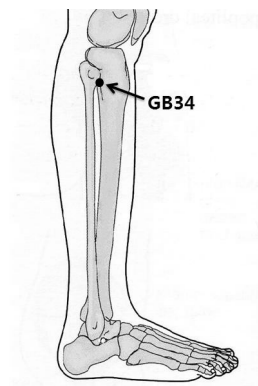


Fig. 2. Stimulations during fMRI scanning were performed at GB34 on the right leg according to the WHO Standard Acupuncture Point Locations of GB34.

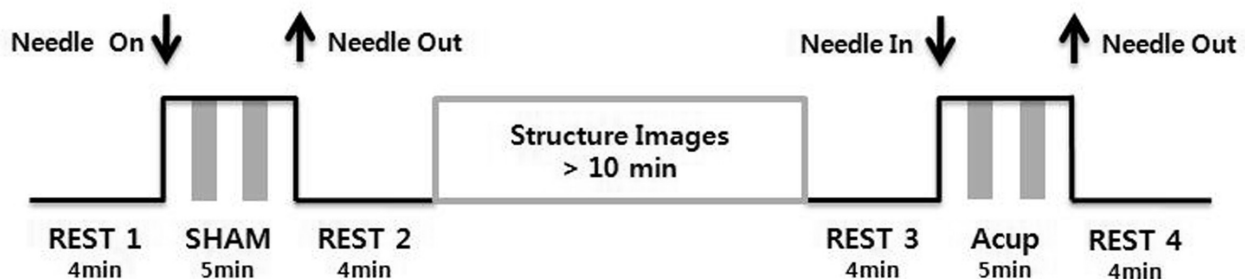


Fig. 1. The fMRI scanning paradigm started with a “REST” condition of 4 min.

There were different blocks of 60 s, during which either passive acupuncture (white block) or active acupuncture (grey block) performed. Afterwards, another “REST” period followed. Between SHAM and ACUP, structure images were acquired.

acquisition voxel size=2.4×2.4×4.5 mm) were collected. During scanning, participants remained in the supine position with their heads immobilized by cushioned supports and wore ear plugs throughout the experiment to attenuate MRI gradient noise. Moreover, they were instructed to rest with their eyes closed and not to move. For spatial normalization and localization, a high resolution T1-weighted anatomical image was then acquired using a magnetization prepared gradient echo sequence (time repetition [TR]=9.9 ms, time echo [TE]=4.6 ms, flip angle=90°, slice thickness=1 mm, matrix=236×240, field of view [FOV]=235×235×196 mm, acquisition voxel size=1×1×1 mm). SPM5 was used (Wellcome Department of Cognitive Neurology, London, UK) implemented in MATLAB 7.4.0 (The MathWorks, Natick, MA) for data preprocessing and statistical analysis. The first five volumes of each participant's dataset were discarded to allow for T1 equilibration. The functional EPI-BOLD images were realigned, and the subject-mean functional MR images were co-registered with the corresponding structure MR images. All the images were normalized to the standard SPM5 template.

## 5. Data analysis

Kendal coefficient of concordance (KCC)<sup>13,18)</sup> was used for measuring the similarity of the time series within a functional cluster based on the regional homogeneity hypothesis<sup>18)</sup>. In the current study, the 27 nearest neighboring voxels were defined as a cluster and a KCC value (range 0~1) was given to the voxel at the center of this cluster. A custom software routine, Resting-State fMRI Data Analysis Toolkit (REST, <http://resting-fmri.sourceforge.net>) was used for ReHo analysis in a voxel-wise fashion. For all participants, the ReHo map was spatially smoothed with 9 mm of full width at half maximum (FWHM).

ALFF<sup>25)</sup> is calculated as the sum of amplitudes within a specific low frequency range. Using Resting-State fMRI Data Analysis Toolkit (REST, <http://resting-fmri.sourceforge.net>), the time course of each voxel was transformed to the frequency domain, and ALFF was calculated as the amplitude integral over a frequency range of 0.01~0.08 Hz. For all

participants, the ALFF map was spatially smoothed with 9 mm of FWHM.

Paired *t*-tests were conducted in order to investigate which areas of the brain were changed after ACUP or SHAM using SPM5. In these analyses, the threshold was a corrected cluster level  $p < 0.05^{26)}$ .

## Results

The results from the group analysis are shown in Fig. 3.

### 1. ReHo maps

Group maps of after-before ACUP demonstrated at the left and right middle frontal gyrus (BA 6, 46), left and right inferior frontal gyrus (BA 13/46/47), left medial frontal gyrus (BA 6, 10), left superior frontal gyrus (BA 6/8/9), left precuneus (BA 31), left angular gyrus (BA 39), left caudate body, left putamen, left anterior cingulate (BA 32), left thalamus, left cingulate gyrus (BA 31), right insula (BA 13), right superior frontal gyrus (BA 6/8/10/11), right inferior frontal gyrus (BA 13/46/47) and right posterior cingulate (BA 30).

Group maps of after-before SHAM showed at the left and right precuneus (BA 7/19), left and right cuneus (BA 17/18), left and right lingual gyrus (BA 18), left and right cerebellum, left superior parietal lobule (BA 7), right postcentral gyrus (BA 3) and right paracentral lobule (BA 6).

Only the left precuneus is shown in both after ACUP and SHAM.

### 2. ALFF

After-before ACUP, the left and right middle frontal gyrus (BA 6/8), left and right medial frontal gyrus (BA 8/10/11), left and right superior temporal gyrus (BA 13/22/39), left and right cerebellum, left superior frontal gyrus (BA 8), right middle temporal gyrus (BA 39), right posterior cingulate (BA 30/31), right fusiform gyrus (BA 37), right precuneus (BA 39), right cingulate gyrus (BA 31), right caudate head, right putamen, right lingual gyrus (BA 19) and right parahippocampal gyrus (BA 27) were demonstrated.

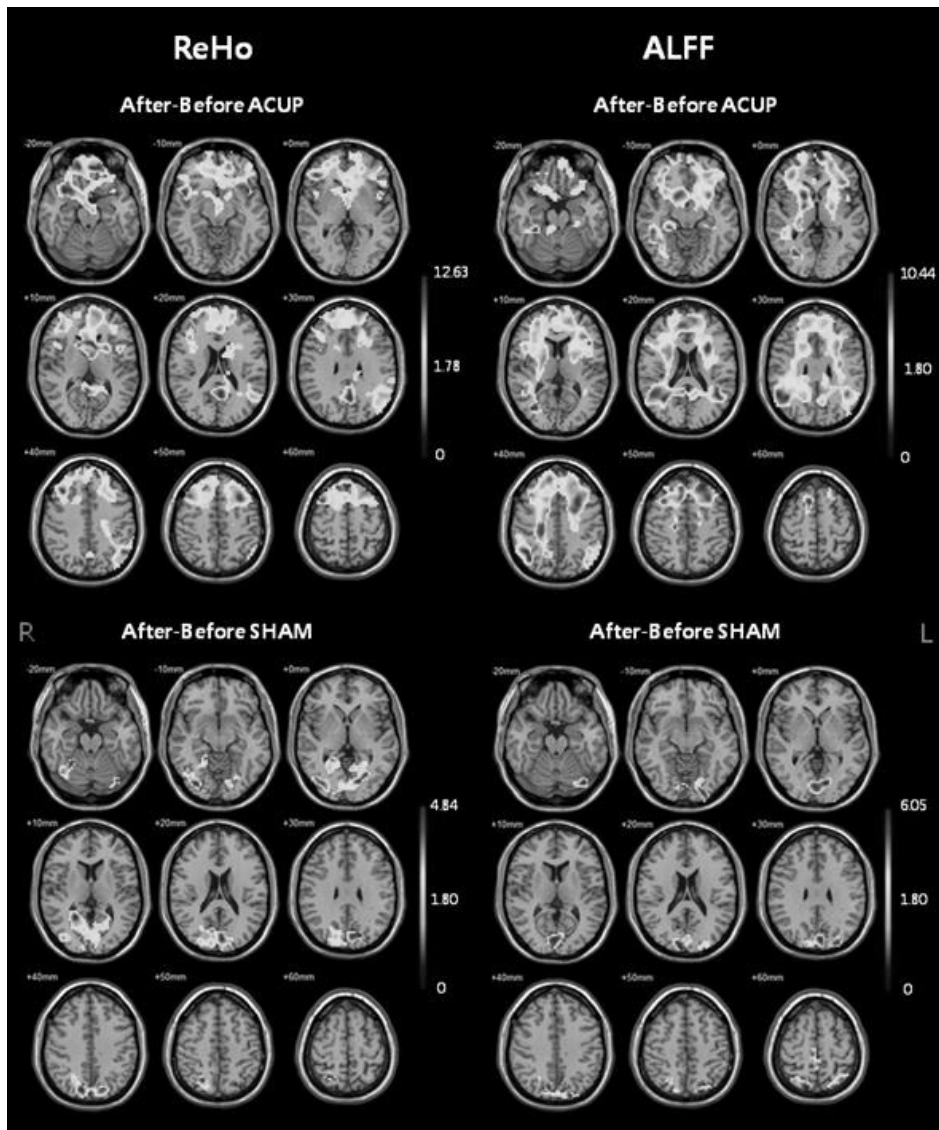


**Fig. 3. Changes in functional connectivity of ReHo and ALFF for ACUP and SHAM (after-before).** Paired *t*-tests were conducted and the threshold was corrected cluster level  $p < 0.05$ . The bar is the *t* value. Note that R = right hemisphere, whereas L = left hemisphere.

After-before SHAM, the left and right cuneus (BA 7/17/18/30), left parahippocampal gyrus (BA 30), left fusiform gyrus (BA 19), left lingual gyrus (BA 18), left cerebellum, right posterior cingulate (BA 30), right precuneus (BA 7) and right middle occipital gyrus (BA 18/19) were shown.

Left cerebellum, right posterior cingulate and right precuneus were demonstrated both after ACUP and SHAM, whereas the other areas were different (Table 1).

## Discussion

A baseline or control state is fundamental to the understanding of most complex systems. A default functionality of the human brain, as revealed by task-independent decreases in activity, occurring during goal-directed behaviors, suggests the existence of an organized, baseline default mode of brain function that is suspended during specific goal-directed behaviors<sup>27,28</sup>. Previous research showed that a set of brain regions, including: PCC, medial prefrontal cortex (MPFC), thalamus, and insula demonstrated higher cerebral blood flow than the whole brain average in the resting state<sup>27</sup>.

Table 1. Group Paired *t*-test Maps of Regional Homogeneity (ReHo) and Amplitude of Low Frequency Fluctuation (ALFF)\*

Regions	ReHo					ALFF				
	Talairach					Talairach				
	x	y	z	<i>t</i> value	BA <sup>†</sup>	x	y	z	<i>t</i> value	BA <sup>†</sup>
<b>ACUP</b>										
Frontal cortex										
Left SFG	-24	15	62	6.85	6/8/9	-18	25	47	5.96	8
Right SFG	21	48	42	7.86	6/8/10/11					
Left MFG	-29	11	48	12.63	6	-26	6	42	6.46	6
Right MFG	32	4	59	9.97	6/46	32	8	49	4.94	6/8
Left MedFG	-16	8	53	6.03	6/10	-4	59	13	5.99	8/10/11
Right MedFG	13	43	38	5	8					
Left IFG	-26	25	-7	4.31	47					
Right IFG	33	14	-10	6.62	13/46/47					
Temporal cortex										
Left STG						-40	-51	15	5.57	13/22
Right STG						48	-55	30	7.08	39
Right MTG						37	-58	32	10.44	39
Right FG						46	-40	-10	6.67	37
Parietal cortex										
Left AG	-49	-61	33	5.79	39					
Left PCu	-4	-60	26	6.52	31					
Right PCu						34	-67	34	6.26	39
Limbic cortex										
Left AC	-1	33	24	4.52	32					
Right PC	1	-51	13	5.43	30	29	-70	9	7.25	30/31
Left CG	-21	-22	40	3.46	31					
Right CG						21	-31	40	5.92	31
Occipital cortex										
Right LG						27	-67	4	5.06	19
Subcortical										
Right Insula	44	7	-5	7.9	13					
Left Pu	-23	6	15	4.81	-					
Right Pu						16	7	5	5.47	-
Left Th	-4	-2	9	4.13	-					
Left Cb	-18	5	18	5.78	-					
Right Ch						10	10	-5	5.51	-
Right Gh						21	-35	-4	4.88	27
Left Cer						-26	-59	-40	4.73	-
Right Cer						21	-52	-30	6.5	-
<b>SHAM</b>										
Frontal cortex										
Right PCL	4	-32	58	3.17	6					
Parietal cortex										
Left SPL	-32	-66	54	3.09	7					
Right PCG	12	-36	69	3.67	3					
Left PCu	-21	-84	39	4.52	7/19					
Right PCu	4	-52	59	4.84	7/19	20	-65	47	4.94	7
Limbic cortex										
Right PC						18	-53	8	6.05	30
Occipital cortex										
Right MOG						35	-81	5	4.04	18/19
Left Cu	-1	-81	10	3.05	18	-18	-78	32	4.12	7/17/18
Right Cu	10	-88	15	3.27	18	7	-70	9	3.58	30
Left LG	-12	-74	-3	3.42	18	-15	-77	-3	3.58	18
Right LG	2	-89	-1	3.06	18					
Left FG						-23	-66	-5	3.38	19
Subcortical										
Left Gh						-23	-50	5	3.24	30
Left Cer	-34	-73	-19	3.46	-	-34	-72	-25	3.72	-
Right Cer	2	-80	-9	3.88	-					

\*The table describes the location of the peak voxel and the corresponding brain regions and Brodmann areas, <sup>†</sup>Brodman area. AC : anterior cingulate, AG : angular gyrus, Cb : caudate body, Ch : caudate head, Cer : cerebellum, CG : cingulate gyrus, Cu : cuneus, FG : fusiform gyrus, Gh : parahippocampal gyrus, IFG : inferior frontal gyrus, LG : lingual gyrus, MedFG : medial frontal gyrus, MFG : middle frontal gyrus, MOG : middle occipital gyrus, MTG : middle temporal gyrus, PC : posterior cingulate, PCG : postcentral gyrus, PCL : paracentral lobule, PCu : precuneus, Pu : putamen, SFG : superior frontal gyrus, SPL : superior parietal lobule, STG : superior temporal gyrus, Th : thalamus. The threshold was corrected cluster level  $p < 0.05$ . The voxel size was  $2.4 \times 2.4 \times 4.5$  mm.

Recent studies showed that this default mode network could be modulated by acupuncture stimulation<sup>13</sup>. Consistent with these results that were obtained with ICA, the hypothesis in the present study was that acupuncture could modulate the resting state not only with ICA, but also with ReHo and ALFF. As can be seen in Table 1, after ACUP, for both ReHo and ALFF, a significantly increased connectivity was found in the; left and right middle frontal gyrus, left medial frontal gyrus, left superior frontal gyrus, and right PCC. Results from the group analysis are shown in Fig. 3. In ReHo, but not ALFF, activations of; left and right inferior frontal gyrus, left precuneus, left angular gyrus, left caudate body, left putamen, left ACC, left thalamus, left cingulate gyrus, right insula, and right superior frontal gyrus were significantly increased. In ALFF, but not ReHo, activations of left superior temporal gyrus, left cerebellum, right middle temporal gyrus, right superior temporal gyrus, right fusiform gyrus, right precuneus, right cingulate gyrus, right caudate head, right putamen, right lingual gyrus, right medial frontal gyrus, right parahippocampal gyrus, and right cerebellum were significantly increased.

After SHAM, for both ReHo and ALFF, an increased connectivity was found in the; left and right cuneus, left lingual gyrus, left cerebellum, and right precuneus. Moreover, in ReHo, but not in ALFF, left precuneus, left superior parietal lobule, right postcentral gyrus, right paracentral lobule, and right lingual gyrus were significantly more activated. Finally, in ALFF, but not ReHo significantly more activation was found in the; left fusiform gyrus, left parahippocampal gyrus, right posterior cingulate, and right middle occipital gyrus.

In previous studies with ICA, the regions of PCC, medial prefrontal cortex, thalamus and insula<sup>27</sup>, inferior parietal lobule, medial areas of the inferior, middle, and superior frontal gyrus<sup>13</sup>, and precuneus<sup>14</sup> were supposed as a default mode network for healthy participants. In addition, higher within-region local synchrony than in other brain regions were found in the; PCC, MPFC, insula, superior temporal gyrus, and thalamus<sup>21</sup>.

For ReHo, our group maps of after-before ACUP demonstrated increased homogeneity in the; left and right middle

frontal gyrus, left and right inferior frontal gyrus, left and right superior frontal gyrus, left precuneus, left thalamus, right insula, and right posterior cingulate. ReHo supposes that voxels within a functional brain area are more temporally homogeneous when this area is involved in a specific condition<sup>18</sup>. ReHo measures the regional homogeneity, which reflects local synchrony by calculating similarity of dynamic fluctuations of voxels within a given cluster. This method is based on observations that meaningful fMRI activity is more likely to occur in clusters of several spatially contiguous voxels than in a single voxel<sup>29,30</sup>. It assumes that within a functional cluster, the hemodynamic characteristics of every voxel would be similar or synchronous with that of its neighbors; and such similarity could be changed or modulated by different conditions. In our study, it was found that acupuncture stimulation can change ReHo of brain regions related to a default mode network.

A previous study reported that high ALFF of cerebral blood flow (CBF) fluctuations were shown in the; PCC, MPFC, insula, superior temporal gyrus, and thalamus<sup>21</sup>. After-before ACUP, increased *t* maps of right PCC, left and right middle frontal gyrus, left superior frontal gyrus, and left and right superior temporal gyrus were demonstrated in ALFF analysis. ALFF<sup>25</sup> was adopted in the current study to depict the local intensity of CBF fluctuations. Previous studies have shown that the low frequency fluctuation (<0.08 Hz) was highly coherent among brain regions during resting state and the spatial pattern of the correlation was quite similar to the activation pattern of tasks<sup>20,31</sup>. The low frequency fluctuations of the resting-state fMRI signal were suggested to reflect spontaneous neuronal activity<sup>32</sup>. Our results showed, in line with previous studies, that PCC and MPFC demonstrated higher cerebral blood flow than the whole brain average in the resting state as an element of a default mode network<sup>27,33</sup>, moreover, it was found that the same areas were modulated by acupuncture stimulation<sup>16</sup>.

In this study, the question; which method (ReHo or ALFF) is most suitable for future clinical neuroimaging studies on acupuncture, for instance, for studies on pain modulation<sup>7</sup>, was the most important one. Much acupuncture research

focuses on various pain problems<sup>34)</sup> and there is evidence that acupuncture can be effective against pain<sup>35)</sup>. In EEG studies, it was found that acupuncture can modulate painful somatosensory evoked potential amplitudes at both short and long latencies after stimulation<sup>36)</sup>. In addition, neuroimaging data showed that acupuncture modulates brain responses in SI, SII, ACC, PFC, insula, thalamus, hypothalamus, amygdala, and hippocampus<sup>37)</sup>, and that decreased pain rating was accompanied by decreased brain activity in the; insula, ACC, and thalamus<sup>38,39)</sup>. Interestingly, a recent neuroimaging study on acupuncture stimulation (also on GB 34), showed brain activations in the same areas as in our study<sup>40)</sup>. As can be seen in Table 1, we found a significant change in the insula, ACC, and thalamus as well, however, only in ReHo. For ALFF, no significant change was found in these areas. Although more future studies with ReHo and ALFF will be needed before any firm conclusions can be drawn, our study shows that particularly ReHo could be an interesting method for future clinical neuroimaging studies on acupuncture.

Limitation of current study is that the actual order of paradigm was SHAM first and ACUP second. Even if we employed washout time, more than 10 min, it could have an order effect. We demonstrated neural changes induced by acupuncture only on GB 34, however, different acupuncture points may appear different. So, verification through research on the several acupoints is required.

## Conclusion

In this study, in which a multi-method approach was used, it was shown that acupuncture can modulate post-stimulus rest. Moreover, it was found that ReHo and ALFF are suitable methods in order to better understand the changes in the resting-state brain network induced by acupuncture. In addition, support is found for the hypothesis that acupuncture stimulation can modulate the default mode network. Finally, our study shows that particularly ReHo could be an interesting method for future clinical neuroimaging studies on acupuncture.

## Acknowledgements

This work was supported by the National Research Foundation of Korea(NRF) grant funded by the Korea government(MSIP)(No. 2007-0054931).

## References

1. Cristian A, Katz M, Cutrone E, Walker RH. Evaluation of acupuncture in the treatment of Parkinson's disease: a double-blind pilot study. *Mov Disord.* 2005 ; 20 : 1185-8.
2. Siedentopf CM, Golaszewski SM, Mottaghy FM, Ruff CC, Felber S, Schlager A. Functional magnetic resonance imaging detects activation of the visual association cortex during laser acupuncture of the foot in humans. *Neurosci Lett.* 2002 ; 327 : 53-6.
3. Liang XB, Luo Y, Liu XY, Lu J, Li FQ, Wang Q, et al. Electro-acupuncture improves behavior and upregulates GDNF mRNA in MFB transected rats. *Neuroreport.* 2003 ; 14 : 1177-81.
4. Park HJ, Lim S, Joo WS, Yin CS, Lee HS, Lee HJ, et al. Acupuncture prevents 6-hydroxydopamine-induced neuronal death in the nigrostriatal dopaminergic system in the rat Parkinson's disease model. *Exp Neurol.* 2003 ; 180 : 93-8.
5. Lee MS, Shin BC, Kong JC, Ernst E. Effectiveness of acupuncture for Parkinson's disease: a systematic review. *Mov Disord.* 2008 ; 23 : 1505-15.
6. Wu MT, Sheen JM, Chuang KH, Yang P, Chin SL, Tsai CY, et al. Neuronal specificity of acupuncture response: a fMRI study with electroacupuncture. *Neuroimage.* 2002 ; 16 : 1028-37.
7. Hui KK, Liu J, Makris N, Gollub RL, Chen AJ, Moore CI, et al. Acupuncture modulates the limbic system and subcortical gray structures of the human brain: evidence from fMRI studies in normal subjects. *Hum Brain Mapp.* 2000 ; 9 : 13-25.
8. Ng DK, Chow PY, Ming SP, Hong SH, Lau S, Tse D, et al. A double-blind, randomized, placebo-controlled trial of acupuncture for the treatment of childhood persistent allergic rhinitis. *Pediatrics.* 2004 ; 114 : 1242-7.
9. Price DD, Rafii A, Watkins LR, Buckingham B. A psychophysical analysis of acupuncture analgesia. *Pain.* 1984 ; 19 : 27-42.
10. Martuzzi R, Ramani R, Qiu M, Rajeevan N, Constable RT.



- Functional connectivity and alterations in baseline brain state in humans. *Neuroimage*. 2009 ; 49 : 823-34.
11. van Eimeren T, Monchi O, Ballanger B, Strafella AP. Dysfunction of the default mode network in Parkinson disease: a functional magnetic resonance imaging study. *Arch Neurol*. 2009 ; 66 : 877-83.
  12. Bai L, Qin W, Tian J, Liu P, Li L, Chen P, et al. Time-varied characteristics of acupuncture effects in fMRI studies. *Hum Brain Mapp*. 2009 ; 30 : 3445-60.
  13. Dhond RP, Yeh C, Park K, Kettner N, Napadow V. Acupuncture modulates resting state connectivity in default and sensorimotor brain networks. *Pain*. 2008 ; 136 : 407-18.
  14. Liu P, Zhang Y, Zhou G, Yuan K, Qin W, Zhuo L, et al. Partial correlation investigation on the default mode network involved in acupuncture: an fMRI study. *Neurosci Lett*. 2009 ; 462 : 183-7.
  15. Greicius MD, Srivastava G, Reiss AL, Menon V. Default-mode network activity distinguishes Alzheimer's disease from healthy aging: evidence from functional MRI. *Proc Natl Acad Sci U S A*. 2004 ; 101 : 4637-42.
  16. Zhang Y, Qin W, Liu P, Tian J, Liang J, von Deneen KM, et al. An fMRI study of acupuncture using independent component analysis. *Neurosci Lett*. 2009 ; 449 : 6-9.
  17. Yeo S, Lim S, Choe IH, Choi YG, Chung KC, Jahng GH, et al. Acupuncture stimulation on GB34 activates neural responses associated with Parkinson's disease. *CNS Neurosci Ther*. 2012 ; 18 : 781-90.
  18. Zang Y, Jiang T, Lu Y, He Y, Tian L. Regional homogeneity approach to fMRI data analysis. *Neuroimage*. 2004 ; 22 : 394-400.
  19. Fransson P. Spontaneous low-frequency BOLD signal fluctuations: an fMRI investigation of the resting-state default mode of brain function hypothesis. *Hum Brain Mapp*. 2005 ; 26 : 15-29.
  20. Biswal B, Yetkin FZ, Haughton VM, Hyde JS. Functional connectivity in the motor cortex of resting human brain using echo-planar MRI. *Magn Reson Med*. 1995 ; 34 : 537-41.
  21. Zou Q, Wu CW, Stein EA, Zang Y, Yang Y. Static and dynamic characteristics of cerebral blood flow during the resting state. *Neuroimage*. 2009 ; 48 : 515-24.
  22. Wu T, Long X, Zang Y, Wang L, Hallett M, Li K, et al. Regional homogeneity changes in patients with Parkinson's disease. *Hum Brain Mapp*. 2009 ; 30 : 1502-10.
  23. Oldfield RC. The assessment and analysis of handedness: the Edinburgh inventory. *Neuropsychologia*. 1971 ; 9 : 97-113.
  24. Lim S. WHO Standard Acupuncture Point Locations. *Evid Based Complement Alternat Med*. 2010 ; 7 : 167-8.
  25. Zang YF, He Y, Zhu CZ, Cao QJ, Sui MQ, Liang M, et al. Altered baseline brain activity in children with ADHD revealed by resting-state functional MRI. *Brain Dev*. 2007 ; 29 : 83-91.
  26. Mezer A, Yovel Y, Pasternak O, Gorfine T, Assaf Y. Cluster analysis of resting-state fMRI time series. *Neuroimage*. 2009 ; 45 : 1117-25.
  27. Raichle ME, MacLeod AM, Snyder AZ, Powers WJ, Gusnard DA, Shulman GL. A default mode of brain function. *Proc Natl Acad Sci U S A*. 2001 ; 98 : 676-82.
  28. Raichle ME, Snyder AZ. A default mode of brain function: a brief history of an evolving idea. *Neuroimage*. 2007 ; 37 : 1083-90; discussion 97-9.
  29. Katanoda K, Matsuda Y, Sugishita M. A spatio-temporal regression model for the analysis of functional MRI data. *Neuroimage*. 2002 ; 17 : 1415-28.
  30. Tononi G, McIntosh AR, Russell DP, Edelman GM. Functional clustering: identifying strongly interactive brain regions in neuroimaging data. *Neuroimage*. 1998 ; 7 : 133-49.
  31. Fox MD, Snyder AZ, Vincent JL, Corbetta M, Van Essen DC, Raichle ME. The human brain is intrinsically organized into dynamic, anticorrelated functional networks. *Proc Natl Acad Sci U S A*. 2005 ; 102 : 9673-8.
  32. Lu H, Zuo Y, Gu H, Waltz JA, Zhan W, Scholl CA, et al. Synchronized delta oscillations correlate with the resting-state functional MRI signal. *Proc Natl Acad Sci U S A*. 2007 ; 104 : 18265-9.
  33. Bluhm RL, Miller J, Lanius RA, Osuch EA, Boksman K, Neufeld RW, et al. Spontaneous low-frequency fluctuations in the BOLD signal in schizophrenic patients: anomalies in the default network. *Schizophr Bull*. 2007 ; 33 : 1004-12.
  34. NIH Consensus Conference. Acupuncture. *JAMA*. 1998 ; 280 : 1518-24.
  35. Staud R. Mechanisms of acupuncture analgesia: effective therapy for musculoskeletal pain? *Curr Rheumatol Rep*. 2007 ; 9 : 473-81.
  36. Xu X, Shibasaki H, Shindo K. Effects of acupuncture on somatosensory evoked potentials: a review. *J Clin Neurophysiol*. 1993 ;

- 10 : 370-7.
37. Wager TD, Rilling JK, Smith EE, Sokolik A, Casey KL, Davidson RJ, et al. Placebo-induced changes in fMRI in the anticipation and experience of pain. *Science*. 2004 ; 303 : 1162-7.
38. Peyron R, Laurent B, Garcia-Larrea L. Functional imaging of brain responses to pain. A review and meta-analysis (2000). *Neurophysiol Clin*. 2000 ; 30 : 263-88.
39. Casey KL. Forebrain mechanisms of nociception and pain: analysis through imaging. *Proc Natl Acad Sci U S A*. 1999 ; 96 : 7668-74.
40. Chae Y, Lee H, Kim H, Kim CH, Chang DI, Kim KM, et al. Parsing brain activity associated with acupuncture treatment in Parkinson's diseases. *Mov Disord*. 2009 ; 24 : 1794-802.

## 국문초록

**목적** : 침치료는 침자극을 가한 뒤, 발침한 뒤에 효과를 나타낸다. 그러므로 침연구에 있어서 침자극을 가하고 발침한 뒤에 나타나는 침의 반응을 관찰하여야 할 필요가 있다. 이에 본 연구에서는 안정성 네트워크를 이용하여 침자극 후의 반응을 관찰하여 발침 후에 뇌에 미치는 침의 반응을 관찰하였다. **방법** : 침자극에 의하여 나타나는 안정성 네트워크의 변화를 관찰하기 위하여 기능성 자기공명 영상장치를 사용하여 12 명의 건강인을 대상으로 우측 양릉천 혈자리에 자침한 후, 침자극 전후의 뇌를 촬영하였다. 그리고 regional homogeneity(ReHo)와 amplitude of low frequency fluctuation(ALFF)를 이용하여 데이터를 분석하였다. **결과** : ReHo와 ALFF에서 공통적으로 안정성 네트워크가 증가된 영역은 좌우측 중전두이랑, 좌측 내측전두이랑, 좌측 상전두이랑, 그리고 우측 뒤쪽 띠이랑의 뇌부위였다. 특히 ReHo분석 결과 섬엽, 앞쪽 띠이랑과 선조체에서 안정성 네트워크가 증가된 것이 관찰되었는데, 이들 영역은 침의 진통작용과 관련된 영역들이다. 하지만 ALFF 분석결과에서는 이들 영역들이 나타나지 않았다. **결론** : ReHo와 ALFF 모두에서 침자극에 의한 안정성 네트워크의 변화를 관찰할 수 있었다. 또한 ReHo분석을 통하여 침자극에 의한 진통관련 영역들의 반응을 관찰할 수 있었다.